Lagrangian statistics in forced two-dimensional turbulence

O. Kamps and R. Friedrich
Institute of Theoretical Physics, University of Münster, Wilhelm-Klemm-Strasse 9, 48149 Münster, Germany
(Received 10 October 2007; revised manuscript received 20 June 2008; published 23 September 2008)

We report on simulations of two-dimensional turbulence in the inverse energy cascade regime. Focusing on the statistics of Lagrangian tracer particles, scaling behavior of the probability density functions of velocity fluctuations is investigated. The results are compared to the three-dimensional case. In particular an analysis in terms of compensated cumulants reveals the transition from a strong non-Gaussian behavior with large tails to Gaussianity. The reported computation of correlation functions for the acceleration components sheds light on the underlying dynamics of the tracer particles.

DOI: 10.1103/PhysRevE.78.036321 PACS number(s): 47.27.−i, 47.10.ad

INTRODUCTION

In recent years, the Lagrangian description of turbulent flows has attracted much interest from the experimental point of view [1,2] as well as in numerical [3,4] and analytical investigations [5]. This is not only due to the relevance of the Lagrangian approach for applications such as turbulent mixing and the dispersion of pollutants. But fundamental turbulence research also benefits from this alternative description and its relation to the Eulerian formulation. The classical Kolmogorov theory (K41) predicts self-similar scaling of the probability density functions (PDFs) of the velocity increments in homogeneous isotropic turbulent flows. It is a well known fact that in three dimensions the assumption of self-similarity is violated for Eulerian velocity increments. This is referred to as Eulerian intermittency [6]. We know from recent experiments [1,2] and numerical simulations [3,4] that intermittency is observed in the Lagrangian picture as well. For two-dimensional turbulence the situation is different: although numerical investigations show deviations from Gaussianity [7] for the Eulerian velocity increments, the inverse cascade provides an Eulerian flow field with scaling properties compatible with the K41 predictions. For this reason, the inverse energy cascade in two-dimensional turbulence seems to be the ideal system to shed light on the Lagrangian statistics and its relation to the Eulerian case.

This paper presents results from numerical investigations of the Lagrangian dynamics of forced two-dimensional turbulence. Thereby we focus on intermittency. The remainder of this article is structured as follows. After briefly discussing the system under consideration and summarizing some facts regarding the numerics, we present results on the Eulerian increment statistics. The main part of the article is devoted to the study of the Lagrangian increment PDFs. Finally we discuss properties of the acceleration correlation.

BASIC EQUATION

The behavior of two-dimensional fluid motion is governed by the vortex transport equation

$$\partial_t \omega = -\boldsymbol{u}\cdot\nabla\omega + \nu\Delta\omega - \gamma\omega - \Delta f, \tag{1}$$

with the vorticity $\omega=\omega(\boldsymbol{x},t)$ and the velocity $\boldsymbol{u}=\boldsymbol{u}(\boldsymbol{x},t)$. The velocity components $u_{x_1}=\partial_{x_2}\phi$ and $u_{x_2}=-\partial_{x_1}\phi$ are connected to the vorticity field ω via the stream function ϕ by $\Delta\phi=-\omega$. We investigate two different types of forcing f. One with a rapidly decaying spatial correlation function $\langle f(\mathbf{x}+\mathbf{r})f(\mathbf{x})\rangle \sim \exp(-r^2/2l_c^2)$ [7], where l_c is the length scale of the correlation. The second is confined to a small shell of wave numbers in Fourier space [8] leading to a long spatial correlation. Both forcings are δ correlated in time and have the property to inject energy at small scales into the system. The forcings are added in Fourier space with constant amplitudes and random phases. In the first case we chose $l_c=0.05$ and in the second case the energy is injected at $k=210$ into the system. The damping term $-\gamma\omega$ in Eq. (1) extracts energy at large scales from the system and avoids the generation of a large scale flow.

NUMERICAL METHOD

The integration of Eq. (1) was performed by a fully dealiased pseudospectral method on a doubly periodic square domain with side length 2π and 1024^2 grid points. For numerical reasons, the viscous term is replaced by a hyperviscous term of order 8. The time evolution for the field and the tracer particles was achieved by a fourth order Runge-Kutta scheme. After reaching stationarity we introduced 10^5 particles with random but equally distributed initial positions

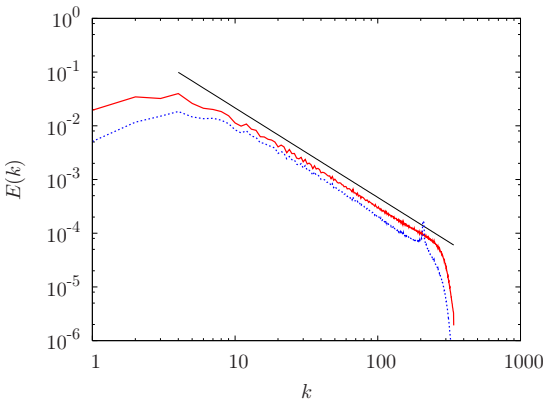

FIG. 1. (Color online) Energy spectra $E(k)$ of simulations using the forcing with the short (upper curve) and the long (lower curve) correlation length. The line denotes the Kolmogorov prediction $E(k)\sim k^{-5/3}$.

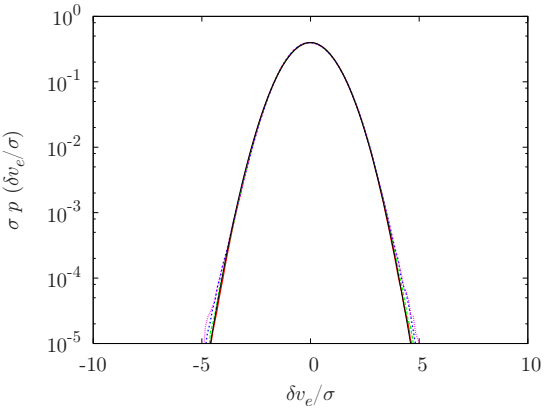

FIG. 2. (Color online) Rescaled PDFs of the Eulerian velocity increments for the distances $r=0.08,0.1,0.2,0.6$. For comparison a Gaussian pdf is shown. Small deviations from Gaussianity exist and can be quantified by the moments [7].

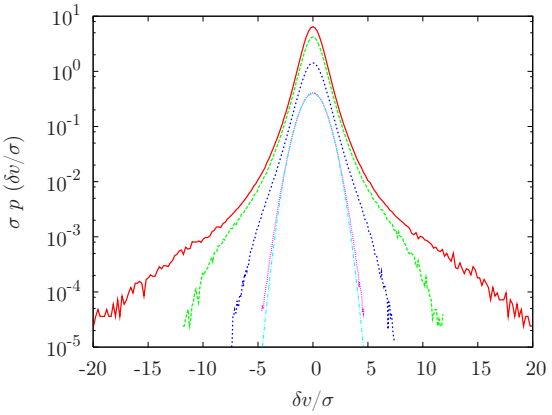

FIG. 3. (Color online) Rescaled PDFs of Lagrangian velocity increments for the time lags $\tau=0.045,0.09,0.22,1.79T_I$ (from outer to inner curves). The most inner curve is a Gaussian pdf. The PDFs are vertically shifted.

into the flow and monitored their trajectories for about 200 Lagrangian integral times T_I. The velocity and the acceleration of the tracers were determined by a bicubic interpolation scheme. Except for Figs. 1 and 7 all presented results are obtained using the forcing with the rapidly decaying spatial correlation.

EULERIAN STATISTICS

In order to check the parameters for the numerical integration, we first analyze the Eulerian velocity field. Figure 1 shows the energy spectrum for both kinds of forcing together with a line showing the K41-scaling $k^{-5/3}$. For a stationary velocity field, the longitudinal Eulerian velocity increments are defined as $\delta v_e(\boldsymbol{x},\boldsymbol{r})=\delta \boldsymbol{v}_e(\boldsymbol{x},\boldsymbol{r})\cdot\hat{\boldsymbol{r}}$ with $\delta \boldsymbol{v}_e(\boldsymbol{x},\boldsymbol{r})=\boldsymbol{u}(\boldsymbol{x}+\boldsymbol{r})-\boldsymbol{u}(\boldsymbol{x})$ and $\hat{\boldsymbol{r}}=\boldsymbol{r}/r$. If we additionally assume isotropy and homogeneity of the flow, we can write $\delta v_e(\boldsymbol{x},\boldsymbol{r})=\delta v_e(r)$. The PDFs $p[\delta v_e(r)]$ are scaled to unit standard deviation by $\sigma p[\delta v_e(r)/\sigma]$ with $\sigma=\langle \delta v_e(r)\rangle^{1/2}$. Figure 2 shows the rescaled PDFs for different r. The shape does not vary with r and hence the PDFs are self-similar. This is in agreement with experimental [9] and numerical [7] studies and leads to the conclusion that intermittency is absent in the inverse energy cascade as far as the Eulerian increments are concerned.

LAGRANGIAN VELOCITY STATISTICS

In the Lagrangian frame of reference the velocities are recorded along the trajectories of tracer particles $\mathbf{v}(\mathbf{y},t)=[\mathbf{u}(\mathbf{x},t)]_{\mathbf{x}=\mathbf{X}(\mathbf{y},t)}$, where $\mathbf{y}$ is the starting position of the tracer and $\mathbf{X}(\mathbf{y},t)$ is its current position. Velocity fluctuations are characterized by the PDFs of the Lagrangian velocity increments $\delta v_i(\tau)=v_i(t+\tau)-v_i(t)$, where v_i is the projection of the velocity on one of the coordinate axes with $i=x_1,x_2$. Due to isotropy the statistics does not depend on the chosen axis. Therefore in the following the Lagrangian velocity increment will be denoted as $\delta v(\tau)$. The moments of $p[\delta v(\tau)]$ are known as the structure functions $S_p(\tau)=\langle \delta v(\tau)^p\rangle$. Figure 3 shows PDFs of the Lagrangian velocity increments for several time lags τ. For time lags of the order of T_I, the PDFs are close to a Gaussian distribution whereas for small τ the PDFs show large tails. A rescaling of the distribution functions resulting in a collapse to a universal distribution is not possible. Accordingly, classical Kolmogorov scaling cannot be observed in the Lagrangian frame in contrast to the Eulerian case. Deviations from the Gaussian shape can be quantified by the compensated cumulants $\lambda_n=c_n/\sigma^n$. The c_n are the cumulants connected to the characteristic function $\hat{C}(k)$ of a PDF $P(x)$ by

$$\hat{C}(k)=\exp\left[\sum_n^\infty \frac{c_n}{n!}(ik)^n\right] \tag{2}$$

and σ^2 is the variance (corresponding to c_2).

For a Gaussian distribution all λ_n with an order n higher than 2 vanish. The compensated cumulants can easily be computed from the structure functions S_p. For symmetric PDFs, $\lambda_4=S_4/S_2^2-3$ is the excess kurtosis and the sixth order normalized cumulant reads $\lambda_6=(S_6-15S_4S_2)/S_2^3+30$. In Fig. 4 we see a log-log plot of λ_4 and λ_6. The crucial point is that for a self-similar signal the kurtosis should be a constant at least in the region where self-similarity of the PDFs is ex-

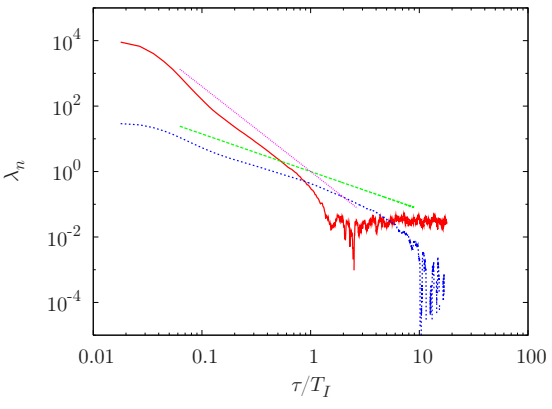

FIG. 4. (Color online) Compensated cumulants of order four (lower curve) and six (upper curve) for 2D turbulence. As a guide for the eye $\tau^{-1.15}$ and $\tau^{-2.6}$ are shown.

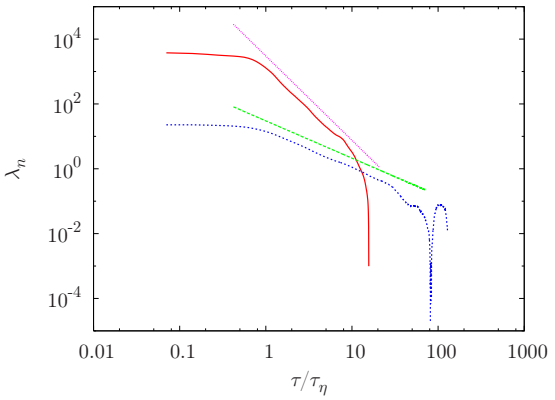

FIG. 5. (Color online) Compensated cumulants of order four (lower curve) and six (upper curve) for 3D turbulence together with $\tau^{-1.15}$ and $\tau^{-2.6}$. The time is given in multiples of the Kolmogorov time τ_η.

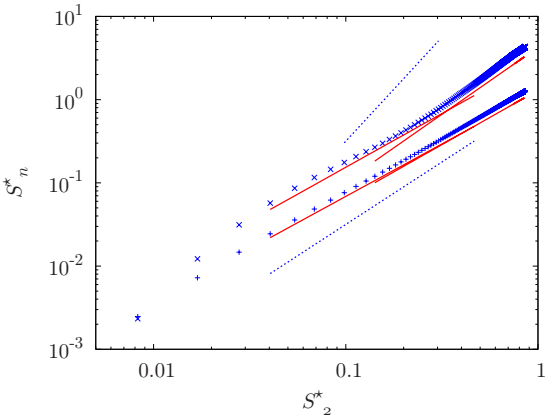

FIG. 6. (Color online) ESS plot of S_3^* (lower curve) and S_5^* (upper curve). The lines show the ESS scaling laws with exponents ζ_p^a (lines ranging from $S_2^*=0.04$ to $S_2^*=0.4$) and ζ_p^b (from $S_2^*=0.015$ to $S_2^*=0.9$) obtained by the two fitting procedures (see text). The dashed lines correspond to the K41 scaling.

pected. In our simulations the kurtosis depends strongly on τ and for intermediate times follows a power law as can be seen in Fig. 4. This also holds for λ_6 which, however, decays faster than λ_4. As a reference we plotted two lines following the power laws $\tau^{-1.15}$ and $\tau^{-2.6}$. During the decay of the cumulants the PDFs converge to the Gaussian shape. In order to investigate the universality of the observed behavior we used the data provided by Refs. [3,10] to calculate the same quantities for three-dimensional turbulence (see Fig. 5). Again scaling behavior can be detected for intermediate times and for comparison we added power laws with the same exponents as in Fig. 4. For very small and very large τ the shapes of the compensated cumulants show differences between 2D and 3D. We devote this to the fact that in 2D the energy is injected on the small scales and mainly dissipated at the large scales whereas in 3D the situation is complementary. Again our results give strong evidence for intermittency in two-dimensional Lagrangian turbulence.

SCALING OF THE LAGRANGIAN STRUCTURE FUNCTIONS

Additionally to the cumulants, the structure functions are computed to characterize the PDFs. As no scaling region is visible for the structure functions we have to rely on the extended self-similarity (ESS) technique [11] in order to estimate scaling exponents. To apply ESS we have to use the structure functions for the absolute values of the velocity increments $S_p^*(\tau)=\langle|\delta v(\tau)|^p\rangle$. Standard arguments of dimensional analysis lead to the scaling behavior $S_p^* \sim \tau^{\zeta_p}$ with $\zeta_p = p/2$. The ESS plot is shown in Fig. 6. Estimating the exponents up to order five in the spirit of Ref. [4] leads to the values ζ_p^a shown in Table I. We also performed the analysis for larger values of S_2^* (corresponding to larger τ) [3] resulting in the exponents ζ_p^b. In both cases the exponents deviate strongly from the K41 predictions which is in agreement with the observation that the excess kurtosis is not constant.

DEPENDENCE ON THE FORCING

To study the effect of the different forcings on Lagrangian observables, we also performed simulations with a forcing limited to a small number of Fourier modes. In this case, the results for the PDFs (Fig. 7) as well as for the cumulants are qualitatively and quantitatively similar to the situation with short spatial correlation. This leads to the conclusion that the observed deviation of the Lagrangian PDFs from the K41 prediction is very robust and seems to be independent of the type of forcing.

ACCELERATION CORRELATIONS

The path of a Lagrangian tracer particle starting at the position $\boldsymbol{y}$ is uniquely defined by the acceleration acting on the particle. The acceleration is given by the right-hand side of the Navier-Stokes equation

$$\boldsymbol{a}(\boldsymbol{y},t) = [-\nabla p(\boldsymbol{x},t) + \nu\Delta\boldsymbol{u}(\boldsymbol{x},t) - \gamma\boldsymbol{u}(\boldsymbol{x},t) + \nabla\times f(\boldsymbol{x},t)]_{\boldsymbol{x}=\boldsymbol{X}(\boldsymbol{y},t)}, \tag{3}$$

where the pressure $p(\boldsymbol{x},t)$ is related to the vorticity by $\Delta p = \nabla\cdot[\boldsymbol{u}\times\boldsymbol{\omega}] - \frac{1}{2}\Delta\boldsymbol{u}^2$. In addition to this fact, the acceleration is also of central interest for turbulence modeling [12,13]. Particularly in two dimensions, it is convenient to split up $\boldsymbol{a}(\boldsymbol{x},t)$ into a component parallel and a component perpendicular to the current velocity of the tracer. The latter is sensitive to circular motions. The two components are defined as $a_\parallel = \boldsymbol{a}\cdot\boldsymbol{u}/|\boldsymbol{u}|$ and $a_\perp = \boldsymbol{a}\cdot(-u_y,u_x)/|\boldsymbol{u}|$. As pointed out in Ref. [14], long correlation times of the velocity increments and the acceleration play a key role for the occurrence of Lagrangian intermittency. This poses the question of whether the observed deviation from self-similarity of the increment PDFs in 2D is also connected to long correlation times of the

TABLE I. ESS scaling exponents for 2D turbulence.

p	1	3	4	5
ζ_p^a	0.557 ± 0.002	1.267 ± 0.007	1.35 ± 0.018	1.313 ± 0.033
ζ_p^b	0.557 ± 0.003	1.313 ± 0.008	1.45 ± 0.019	1.588 ± 0.029

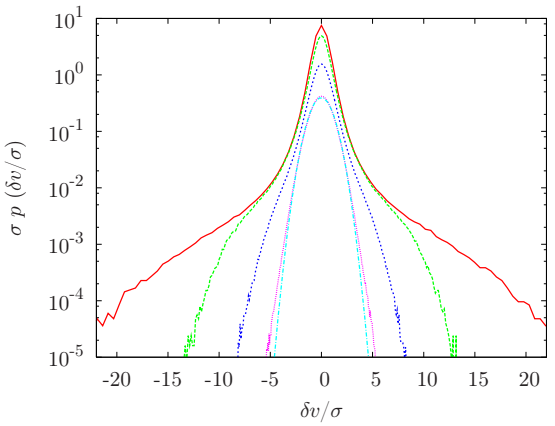

FIG. 7. (Color online) Rescaled PDFs of Lagrangian velocity increments for the same time lags as in Fig. 2. In this case the forcing was confined to a small number of Fourier modes.

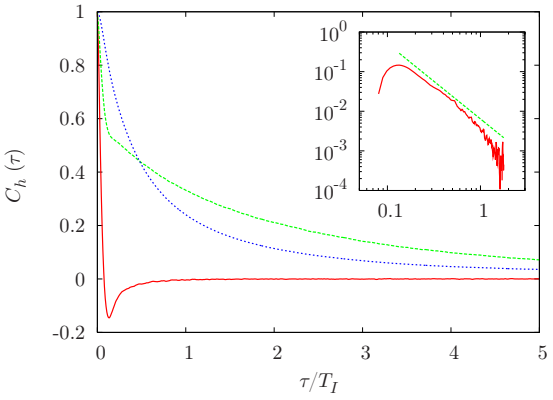

FIG. 8. (Color online) Correlation functions $C_{a_\perp}(\tau)$ (upper curve), $C_{a_\parallel}(\tau)$ (lower curve), and $C_v(\tau)$ (middle curve). The inset presents a log-log plot of $-C_{a_\parallel}(\tau)$. The line corresponds to $\tau^{-1.9}$.

acceleration. In Fig. 8 we can see the correlation functions $C_h(\tau)$ with $h=a_\perp, a_\parallel, \boldsymbol{v}$ for the two components of the acceleration and for the velocity defined as $C_h(\tau)=\langle h(t)h(t+\tau)\rangle/\langle h^2(t)\rangle$. The correlation for the parallel component decays very fast and approaches zero after passing a minimum at negative values. The perpendicular acceleration component also decorrelates very fast for small τ. For τ bigger than the time corresponding to the minimum of $C_{a_\parallel}(\tau)$ it bends off into a region where it decays much slower leading to a very long correlation time. The same behavior is also observed for 3D turbulence [1,15,16]. In Ref. [15] it was related to the spiraling motion in a vortex filament. Here we also observe events where the particle runs through loops. Because the motion is confined to a plane, there is no movement in the third spatial dimension that could contribute to the decorrelation of $a_\perp$. For comparison also $C_{\boldsymbol{v}}$ is shown in Fig. 8. The inset in the same figure demonstrates that $C_{a_\parallel}$ follows a power law in the range between its minimum and T_I. The results for the temporal correlations of the acceleration suggest that the stochastic process for the velocity increments is essentially non-Markovian, as has been emphasized in Ref. [17].

CONCLUSION

We presented a detailed investigation regarding the statistics of tracer particles in the inverse energy cascade regime of two-dimensional turbulence. For different types of forcing, we detect the same deviations from self-similarity for the Lagrangian velocity increment PDFs. This is strong evidence in favor of Lagrangian intermittency in the inverse energy cascade. It is of particular interest as for the Eulerian frame no intermittency can be detected. Any attempt to relate the two frames of reference has to incorporate this fact. The observation that in 2D and 3D the compensated cumulants show the same scaling behavior for intermediate time lags suggest that the underlying dynamical process exhibits a certain degree of universality independent of the dimension. This view is supported by the fact that the acceleration components show long time correlations which are similar to the 3D case. The explanation for the scaling of the compensated cumulants remains an open question.

ACKNOWLEDGMENTS

We are grateful to H. Homann, R. Grauer, and M. Wilczek for fruitful discussions and acknowledge support from the Deutsche Forschungsgesellschaft (Grant No. FR 1003/8-1). We also thank the supercomputing center Cineca (Bologna, Italy) for providing and hosting of the data for 3D turbulence.

[1] A. La Porta, G. Voth, A. M. Crawford, J. Alexander, and E. Bodenschatz, Nature (London) **409**, 1017 (2001).
[2] N. Mordant, P. Metz, O. Michel, and J.-F. Pinton, Phys. Rev. Lett. **87**, 214501 (2001).
[3] L. Biferale, G. Bofetta, A. Celani, A. Lanotte, and F. Toschi, Phys. Fluids **17**, 021701 (2005).
[4] H. Homann, R. Grauer, A. Busse, and W. C. Müller, J. Plasma Phys. **73**, 821 (2007).
[5] R. Friedrich, Phys. Rev. Lett. **90**, 084501 (2003).
[6] U. Frisch,*Turbulence: The Legacy of A. N. Kolmogorov* (Cambridge University, Cambridge, 1996).
[7] G. Boffetta, A. Celani, and M. Vergassola, Phys. Rev. E **61**, R29 (2000).
[8] P.-L. Sulem and U. Frisch, Phys. Fluids **27**, 1921 (1984).
[9] J. Paret and P. Tabeling, Phys. Fluids **10**, 3126 (1998).
[10] L. Biferale, G. Boffetta, A. Celani, B. J. Devenish, A. Lanotte, and F. Toschi, Phys. Rev. Lett. **93**, 064502 (2004).
[11] R. Benzi, S. Ciliberto, R. Tripiccione, C. Baudet, F. Massaioli, and S. Succi, Phys. Rev. E **48**, R29 (1993).
[12] A. K. Aringazin and M. I. Mazhitov, Phys. Rev. E **69**, 026305 (2004).

[13] A. M. Obukhov, Adv. Geophys. **6**, 113 (1959).
[14] N. Mordant, J. Delour, E. Lévêque, A. Arnéodo, and J.-F. Pinton, Phys. Rev. Lett. **89**, 254502 (2002).
[15] L. Biferale and F. Toschi, J. Turbul. **6**, 40 (2005).
[16] N. Mordant, E. Lévêque, and J.-F. Pinton, New J. Phys. **6**, 116 (2004).
[17] R. Friedrich, F. Jenko, A. Baule, and S. Eule, Phys. Rev. Lett. **96**, 230601 (2006).